Three-dimensional structure and decay properties of vortices in shallow fluid layers

Three-dimensional structure and decay properties of vortices in shallow fluid layers

M. P. Satijn and A. W. Cense
Eindhoven University of Technology, Department of Physics, Fluid Dynamics Laboratory, P.O. Box 513, 5600 MB Eindhoven, The Netherlands

R. Verzicco
Politecnico di Bari, Dipartimento di Ingegneria Meccanica e Gestionale, Via Re David 200, 70125 Bari, Italy

H. J. H. Clercx and G. J. F. van Heijst
Eindhoven University of Technology, Department of Physics, Fluid Dynamics Laboratory, P.O. Box 513, 5600 MB Eindhoven, The Netherlands

(Received 9 October 2000; accepted 4 April 2001)

Recently, several laboratory experiments on vortex dynamics and quasi-two-dimensional turbulence have been performed in thin (stratified) fluid layers. Commonly, it is tacitly assumed that vertical motions, giving rise to a three-dimensional character of the flow, are inhibited by the limited vertical dimension. However, shallow water flows, which are vertically bounded by a no-slip bottom and a free surface, necessarily possess a three-dimensional structure due to the shear in the vertical direction. This shear may lead to significant secondary circulations. In this paper, the three-dimensional (3D) structure and the decay properties of vortices in shallow layers of fluid, both homogeneous and stratified, have been studied in detail by 3D direct numerical simulations. The quasi-two-dimensionality of these flows is an important issue if one is interested in a comparison of experiments of this type with purely two-dimensional theoretical models. The influence of several flow parameters, like the depth of the fluid and the Reynolds number, has been investigated. In general, it can be concluded that the flow loses its two-dimensional character for larger fluid depth and larger Reynolds number. Furthermore, it is possible to construct a regime diagram that allows the assessment of the parameter regime, where the flow can be considered as quasi-two-dimensional. It is found that the presence of secondary circulations within a planar vortex flow results in a deformation of the radial profile of axial vorticity. In the limiting case of quasi-two-dimensional flow, the vorticity profiles can be scaled according to a simple diffusion model. In a two-layer stratified system, the decay is reduced and three-dimensional motions are significantly inhibited compared to the corresponding flows in a homogeneous layer. [DOI: 10.1063/1.1374936]

I. INTRODUCTION

The dynamical properties of quasi-two-dimensional (hereafter referred to as Q2D) vortex structures are relevant in the field of geophysical fluid dynamics. Vortices are abundant in nature; well-known geophysical examples are high- and low-pressure cells in the atmosphere and, for instance, Gulf Stream rings and Meddies in the Atlantic Ocean. In order to gain more insight in geophysical flows, vortex dynamics, and two-dimensional turbulence, a large number of numerical studies as well as numerous laboratory experiments have been carried out.

Within the context of geophysical fluid dynamics and two-dimensional turbulence, several types of laboratory experiments have been performed. Depending on the specific phenomena of interest, experiments have been carried out in rotating fluids,[1,2] in stratified environments,[3–5] or in rotating-stratified systems.[6] As for large-scale geophysical flows, the actions of the Coriolis and buoyancy forces tend to two-dimensionalize the flows in these cases. Research on two-dimensional turbulence has also been performed in MHD experiments, where the presence of a homogeneous magnetic field confines the flow to two dimensions. In that case, the action of the Lorentz force is equivalent to the role of the Coriolis force in a rotating system. An example of such an experiment is discussed by Sommeria.[7]

A flow could also be considered as two-dimensional if a significant geometrical confinement is imposed. It is then assumed that the limited vertical dimension will confine the flow to an almost planar one. This argument allows one to study Q2D flows by performing experiments in thin layers of fluid, e.g., experiments in soap films. Several of these studies have been reported in the literature.[8–10] Besides the experiments on soap films, it is also possible to study Q2D flows in a thin layer of fluid inside a container, for example, the experiments on vortex interactions performed by Antonova *et al.*[11] and the experiments on freely decaying Q2D turbulence by Tabeling *et al.*[12] In the latter experiment, but also in several other studies of this type, the flow is forced electromagnetically. Other examples are the experiments on the interaction of allocated vortices performed by Danilov *et al.*[13] and the experimental study of Q2D shear flows by Dolzhan-

skii *et al.*[14,15] In the experimental studies on thin-layer flows of this type, usually a single layer of fluid is used. Recently, in the experiments of Paret and Tabeling,[16] a system of salt-stratified fluid layers was used. The stable two-layer stratification provides an additional mechanism for two-dimensionalization by inhibiting vertical motions.

In every natural flow situation and in every type of laboratory experiment on Q2D flows, three-dimensional effects play an additional role. In a confined rotating system, one encounters the influence of Ekman and Stewartson boundary layers, whereas in a stratified fluid, the presence of internal waves and vertical diffusion mainly account for three-dimensionality. In soap film experiments, the influence of thickness fluctuations and air drag is still an open question.

In Paret *et al.*[17] it was shown that, for the flow parameters used in their experiments, a stratified thin layer configuration can be considered as two dimensional. Supporting evidence was provided by laboratory experiments, although these experiments did not allow full 3D flow measurements. A numerical study concerning Q2D issues in thin-layer experiments was performed by Jüttner *et al.*,[18] but in this case no information was obtained about the full three-dimensional structure of the flow field either.

In this paper, we will focus on a numerical and theoretical analysis of the complete three-dimensional structure and decay properties of such vortex flows. The decay properties are of interest since not only lateral diffusion will play a role, but also vertical diffusion (like in stratified fluids), which is absent in purely 2D flows. Usually, the effect of vertical diffusion in shallow fluid layers is modeled by adding a linear friction term to the two-dimensional Navier–Stokes equation. A similar linear term, of course with different friction coefficients, is used to model the decay in case of Ekman damping in a rotating fluid or the damping by the Hartmann layer in the case of MHD experiments. Note that in these two cases there appears to be a difference with shallow water flows, since for rotating fluids and MHD flows, the linear external friction is asymptotically exact under certain conditions, as was discussed by Dolzhanskii.[19] As yet, it is not completely clear whether this approximation is valid in general for shallow water flows. It is worthwhile to note that it was shown by Dolzhanskii *et al.*[14,15] that the 2D hydrodynamic equation with Rayleigh friction correctly describes the stability of shear flows in thin layers of homogeneous fluid.

The analysis is carried out by performing 3D direct numerical simulations of axisymmetric monopolar vortices in shallow fluid layers. Only decaying vortices will be studied here; the more complex problem of forced vortical flows (e.g., flows driven continuously by electromagnetic forcing) will be discussed in a future study. Two cases will be considered: the case of a vortex in a homogeneous layer of fluid of depth H and the case of a two-layer stratified system, as used in the experiments of Paret *et al.*[16] In both cases, the layers are bounded by a no-slip bottom and a stress-free upper surface. The no-slip condition at the bottom implies a shear in the vertical direction. Although the shear itself leads to a three-dimensional structure of the vortex, it will also set up a secondary circulation. A similar recirculation can be observed where an Ekman boundary layer is present at a no-slip bottom in a rotating system and, for instance, in ''Einstein's tea leaves experiment.'' Depending on the flow parameters, the most important being the depth H of the fluid and the Reynolds number Re, this circulation will vary in strength and its influence will be more or less pronounced. Hence, it is expected that the vortex can be considered as being quasi-two-dimensional only under certain circumstances, which are yet undetermined. Therefore, a regime diagram should be constructed to assess the parameter regime where the quasi-two-dimensionality of such flows is valid. The quasi-two-dimensionality of such flows is an important issue if one wishes to compare experiments of this type with purely two-dimensional theoretical models, or with Q2D models where the bottom friction has been parametrized. Besides this specific motivation, the problem is an interesting one in itself.

The rest of this paper is organized as follows: in Sec. II, a relatively simple, diffusion-based model will be derived to describe the decay and vertical structure of vortices in shallow fluid layers. In Sec. III, we will briefly discuss the numerical simulation method and some other numerical issues. In Sec. IV we present numerical simulations of vortices in a homogeneous layer of fluid for several different fluid depths and Reynolds numbers. The three-dimensional structure will be analyzed and the decay of the vortices will be compared with the model of Sec. II. In Sec. V, some additional simulations are discussed concerning vortices in a two-layer stratified system. Finally, some conclusions are summarized in Sec. VI.

II. AN ANALYTICAL MODEL OF A MONOPOLAR VORTEX IN A SHALLOW FLUID LAYER

Consider a circular monopolar vortex in a shallow layer of fluid, i.e., the vertical dimension H is smaller than the horizontal length scale L, where the domain is vertically bounded by a no-slip bottom and a free surface. It is convenient to describe such a flow in a cylindrical coordinate system (r,θ,z) with corresponding velocities (v_r,v_θ,v_z). Together with axisymmetry, it is assumed that there is no vertical motion, i.e., $v_z=0$. Continuity implies that in this case also $v_r=0$. We are thus left with a quasi-two-dimensional purely azimuthal vortex flow. In terms of the Navier–Stokes equation in cylindrical coordinates this leads to the following partial differential equation for the azimuthal velocity $v_\theta(r,z,t)$:

$$\frac{\partial v_\theta}{\partial t}=\nu\left[\frac{1}{r}\frac{\partial}{\partial r}\left(r\frac{\partial v_\theta}{\partial r}\right)-\frac{v_\theta}{r^2}+\frac{\partial^2 v_\theta}{\partial z^2}\right], \tag{1}$$

with ν the kinematic viscosity.

Apart from this diffusion equation for v_θ, two additional relations, the so-called cyclostrophic and hydrostatic balances, can be derived from the r and z component of the Navier–Stokes equation. These balances will be discussed in the last part of this section. As a first step, the diffusion equation will be solved.

A. Solution of the diffusion equation

The diffusion equation for v_θ is a linear equation that can be solved by a separation of variables, i.e., by assuming that the azimuthal velocity v_θ can be written as $v_\theta(r,z,t)=R(r)Z(z)T(t)$. A similar problem for the decay of vortices in a linearly stratified fluid has been solved recently by Beckers *et al.*,[3] and thus some mathematical aspects of the flow analysis will not be discussed in full detail here. A separation of variables obviously leads to three equations: one for the temporal part $T(t)$, another one for the axial part $Z(z)$, and, finally, one for the radial part $R(r)$ of the solution. The substitution of $v_\theta(r,z,t)=R(r)Z(z)T(t)$ into (1) yields the following three equations for the temporal, axial, and radial part of the problem, respectively:

$$\frac{dT(t)}{dt}=-\nu(p^2+q^2)T(t), \tag{2}$$

$$\frac{d^2Z(z)}{dz^2}=-q^2Z(z), \tag{3}$$

$$\frac{d^2R(r)}{dr^2}+\frac{1}{r}\frac{dR(r)}{dr}-\frac{1}{r^2}R(r)=-p^2R(r), \tag{4}$$

with p^2 and q^2 the separation constants or eigenvalues of the equations. The solution of the temporal equation can be expressed in terms of exponential functions $\exp(-\nu q^2 t)$ and $\exp(-\nu p^2 t)$. When p^2 and q^2 are real, both terms lead to a damping of the velocity field, where the first one is obviously associated with the axial part of the solution, while the second one is related to the radial part of the problem.

Together with the no-slip boundary condition at the bottom ($v_\theta|_{z=0}=0$), the solution of the axial–temporal part $\hat{Z}(z,t)$ of the problem can be formulated in terms of a series of sine solutions with corresponding exponential dampings,

$$\hat{Z}(z,t)=\sum_{n=0}^{\infty} c_n \sin(q_n z)\exp(-\nu q_n^2 t). \tag{5}$$

The eigenvalues of the solution can be found by applying the stress free boundary condition at the upper surface ($\partial v_\theta/\partial z|_{z=H}=0$) and are given by $q_n^2=(2n+1)^2\pi^2/4H^2$, which represents a discrete spectrum of eigenvalues. It will be assumed that only the first mode ($n=0$) of the series is important in the time evolution, since the decay times of the higher-order modes, which are given by $\tau_n=1/\nu q_n^2$, are much smaller. As a consequence, any appropriate vertical profile of an initial distribution of $v_\theta(r,z)$ will soon evolve toward the following solution:

$$Z(z)=\sin\left(\frac{\pi z}{2H}\right), \tag{6}$$

which is a Poiseuille-like profile in the axial direction. The damping associated with the shear is then a single exponential term $\exp(-\pi^2\nu t/4H^2)$. Note that we have taken $c_0=1$, which can be done without loss of generality.

The general solution of the radial–temporal part $\hat{R}(r,t)$ of the problem can be expressed in terms of Bessel functions, and is given by[3]

$$\hat{R}(r,t)=\int_0^\infty a(p)J_1(pr)\exp(-\nu p^2 t)dp, \tag{7}$$

in which $a(p)$ is determined by the initial condition. Being one of the possible solutions, a shielded Gaussian vortex, which turned out to be a useful model in several related previous studies, is taken to solve the problem. Here, a shielded vortex is chosen for the following reason. Vortex lines inside a fluid have to form closed loops or end at a free surface, but they cannot end at a no-slip bottom. (Vortex lines are defined as lines at which at any point the local vorticity vector is directed tangentially, in analogy with streamlines.) In our situation, they will end at the free surface, which means that a patch of single-signed vorticity is always accompanied by an annulus of oppositely signed vorticity. In fact, it is not possible to create a single vortex structure, consisting of a patch of single-signed vorticity. Indeed, in the thin-layer experiment performed by Paireau *et al.*,[20] in which a single vortex subjected to a shear flow was studied, this vortex appeared to be shielded. It is reasonable to assume a Gaussian profile, since this corresponds to a self-similar solution of the two-dimensional diffusion equation. It was shown by Kloosterziel[21] that any appropriate axisymmetric distribution of vorticity with zero net circulation eventually evolves toward this particular profile. The time-dependent velocity profile of this vortex has the following form:

$$\hat{R}(r,t)=\frac{a_0 r}{2(r_0^2+4\nu t)^2}\exp\left(-\frac{r^2}{r_0^2+4\nu t}\right). \tag{8}$$

For this specific profile, $a(p)$, as used in (7), is given by $a(p)=\frac{1}{8}a_0 p^2\exp(-\frac{1}{4}p^2r_0^2)$. The corresponding profile of axial vorticity $\omega_z(r,t)$, the vorticity being defined as $\omega_z=(1/r)(\partial/\partial r)(rv_\theta)$, is given by

$$\omega_z(r,t)=\frac{a_0}{(r_0^2+4\nu t)^2}\left(1-\frac{r^2}{r_0^2+4\nu t}\right)\exp\left(-\frac{r^2}{r_0^2+4\nu t}\right). \tag{9}$$

Note that the equations have been solved in a dimensional form. The quantities a_0 and r_0 in (9) determine the initial amplitude (given by a_0/r_0^2) and radius of the vortex.

It can easily be verified that this vortex is isolated, i.e., it has zero net circulation ($\Gamma=2\pi\int_0^\infty r\omega_z dr=0$). It follows that the decay associated with the radial part of the solution, leads to a decay of the vortex amplitude as $\hat{a}\sim a_0/(r_0^2+4\nu t)^2$ and an increase of its radius as $\hat{r}\sim(r_0^2+4\nu t)^{1/2}$. This part of the decay represents ordinary two-dimensional lateral diffusion. Combining the solutions for the axial–temporal part $\hat{Z}(z,t)$ and radial–temporal part $\hat{R}(r,t)$ yields the full solution of the problem:

$$v_\theta(r,z,t)=\frac{a_0 r}{2(r_0^2+4\nu t)^2}\exp\left(-\frac{r^2}{r_0^2+4\nu t}\right)\sin\frac{\pi z}{2H}\exp(-\lambda t), \tag{10}$$

with $\lambda=\pi^2\nu/4H^2$, sometimes referred to as the external friction parameter. In terms of the 3D vorticity vector $\boldsymbol{\omega}$, this flow field can be described completely by two of its components, $\boldsymbol{\omega}=(\omega_r,0,\omega_z)$, or

$$\boldsymbol{\omega}=\left(-\frac{\partial v_\theta}{\partial z},0,\frac{1}{r}\frac{\partial(rv_\theta)}{\partial r}\right). \tag{11}$$

It follows that the radial component ω_r of the vorticity is associated with the vertical shear $\partial v_\theta/\partial z$, while the axial component ω_z is related to radial gradients in the azimuthal velocity field. The azimuthal component of the vorticity $\omega_\theta = \partial v_r/\partial z - \partial v_z/\partial r = 0$ since $v_r = 0$ and $v_z = 0$.

It can easily be verified that for the solution given by (10), the 3D diffusion operator $\nu\nabla^2_{3D}$ can be rewritten in the following form: $\nu\nabla^2_{3D} = \nu\nabla^2_{2D} - \lambda$. Since the two decay mechanisms, lateral diffusion and additional exponential decay due to vertical diffusion, are now effectively separated, it is possible to define two different Reynolds numbers in this problem: the ordinary Reynolds number $\mathrm{Re} = L^2\omega/\nu$, which is associated with lateral diffusion, and a Reynolds number Re_λ, which is associated with the exponential damping due to vertical diffusion, which is given by $\mathrm{Re}_\lambda = \omega/\lambda$. The quantities ω and L represent typical values for the vorticity and horizontal length scale in the flow, respectively. [In terms of the solution as given by (10), the equations of motion can be made nondimensional by the values of r_0 and a_0.] The three-dimensional Navier–Stokes equation for this problem, using the assumptions made above, could be simplified to the following two-dimensional form:

$$\frac{\partial \mathbf{v}}{\partial t} + (\mathbf{v}\cdot\boldsymbol{\nabla})\mathbf{v} = -\boldsymbol{\nabla} p + \frac{1}{\mathrm{Re}}\nabla^2\mathbf{v} - \frac{1}{\mathrm{Re}_\lambda}\mathbf{v}, \tag{12}$$

where $\mathbf{v}$ is the 2D velocity vector. The bottom friction has now been parametrized by an additional linear term in the 2D Navier–Stokes equation. The friction associated with this term, which obviously results in a nonselective dissipation (with respect to the scales of the flow), is often referred to as ''Rayleigh friction.'' Note that for extremely shallow water flows ($H \ll L$) the decay is completely governed by vertical diffusion. In that case $\mathrm{Re}_\lambda \ll \mathrm{Re}$, which means that the third term on the right-hand side $[(1/\mathrm{Re}_\lambda)\mathbf{v}]$ in (12) will dominate the second one $[(1/\mathrm{Re})\nabla^2\mathbf{v}]$. Note that the formulation of the Navier–Stokes equation as in (12) can be used more generally for shallow water flows. As was mentioned in the Introduction, it is also a commonly used parametrization in studies of Q2D turbulent flows in shallow fluid layers.[12,13] In that case, it could be expected that the behavior and the decay properties of very small scales (so that $H \sim L$) are not described correctly, which could be a drawback of this formulation. This point will be discussed in Sec. IV.

To summarize: Equation (10) describes the time evolution of the velocity field of a shielded vortex in a thin layer of fluid with a Poiseuille-like vertical profile. The solution has an essentially three-dimensional (vertical) structure, but can be considered as quasi-two-dimensional since both $v_r = 0$ and $v_z = 0$.

B. The hydrostatic and cyclostrophic balance, evolution of the free surface

In the previous part of this section, the diffusion equation for v_θ has been solved. The assumptions that were made there ($v_z = 0$ and $v_r = 0$) reduce the radial and axial component of the Navier–Stokes equation to the following relations:

$$-\frac{v_\theta^2}{r} = -\frac{1}{\rho}\frac{\partial p}{\partial r}, \tag{13}$$

$$-\frac{1}{\rho}\frac{\partial p}{\partial z} = g, \tag{14}$$

respectively. The two equations express that the flow should be both in cyclostrophic (13) and hydrostatic (14) balance. Considering these cyclostrophic and hydrostatic balances more carefully, it can be understood that necessarily a secondary circulation in the (r,z) plane should exist. Due to the no-slip condition for v_θ at $z = 0$, the radial pressure gradient force $-(1/\rho)(\partial p/\partial r)$ is no longer balanced by the centrifugal force near the bottom, according to (13). Hence, a flow toward the axis of the vortex is set up there, leading to a recirculation in the (r,z) plane. This results in a nonzero v_r and v_z and thus to nonzero azimuthal vorticity ω_θ.

The presence of secondary circulations is inconsistent with the diffusion model, in which it was assumed that $v_r = 0$ and $v_z = 0$. The inconsistency suggests that the assumptions made in the diffusion model should be slightly relaxed to $v_r, v_z \ll v_\theta$. The recirculation can then be seen as a relatively small perturbation of the basic state, as described by (10). An important issue that remains to be investigated is the parameter regime in which this condition is fulfilled.

From Eq. (13) it also follows that a swirling flow v_θ results in a deformation of the free surface. In several situations, such a deformation can be observed in the form of a dimple, where a vortex tube connects to a free surface. Combining Eq. (13) and $p(r,z) = \rho g[h(r) - z]$, resulting from (14) with $h(r)$ a functional form for the shape of the free surface, relates the deformation of the free surface to the azimuthal velocity field by

$$\frac{1}{gr}v_\theta^2 = \frac{\partial h}{\partial r}. \tag{15}$$

It is thus possible to derive an expression for the evolution of the shape of the free surface in time. Using the velocity profile given by (10) and integrating (15) over the total fluid depth H yields the following approximation for $h(r,t)$:

$$h(r,t) = H - \frac{a_0^2\exp(-2\lambda t)}{32g(r_0^2+4\nu t)^3}\exp\left(-\frac{2r^2}{r_0^2+4\nu t}\right). \tag{16}$$

The solution describes a dimple that slowly broadens in time, and decays due to the two damping mechanisms, as discussed in the previous part of this section. For typical flow conditions, the deformation of the free surface will be very weak, since its amplitude is given by $a_0^2/32g$. It will therefore be left out of consideration in the rest of the paper. To summarize most of the aspects of the vortex discussed so far, Fig. 1 presents a schematic picture of the complete three-dimensional structure of the flow field, including the secondary circulation.

It is the purpose of the numerical simulations that are presented in the next sections to determine whether the sec-

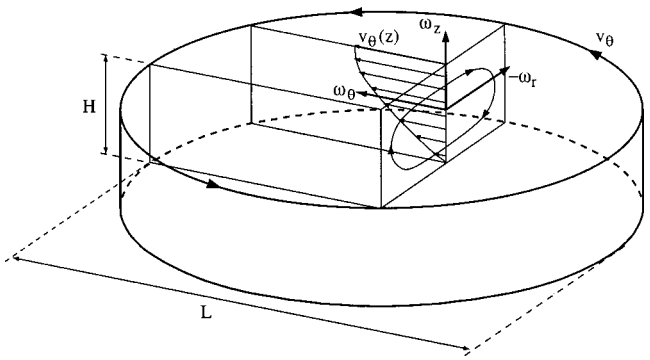

FIG. 1. Schematic picture of the three-dimensional structure of a vortex in a shallow fluid layer.

ondary circulation, as discussed above, is substantial or not. In case that it is large, the Q2D approximation ($v_r, v_z \ll v_\theta$) no longer holds and the parametrization of the friction as in (12) is no longer valid. The influence of the secondary circulations on the evolution of the vortex will also be discussed in more detail.

III. NUMERICAL METHOD

The numerical simulations described in this paper have been performed using a finite difference code in cylindrical coordinates. One of the advantages of this code is the possibility of solving the equations of motion for axisymmetric problems, i.e., the equations are solved in the (r,z) plane. The computational effort is thus significantly reduced, since a two-dimensional numerical problem is solved instead of a fully three-dimensional one.

The equations of motion are solved by using a fractional step method, as described by Verzicco and Orlandi.[22] The velocities (v_r, v_θ, v_z), the pressure p, and the salinity S are discretized on a staggered grid. (Flows in a homogeneous layer as well as flows in a stratified system will be studied.) The pressure and salinity are defined at the centers of the grid cells, whereas the components of the velocity are defined at the centers of the cell boundaries that are perpendicular to the respective velocity components.

Solving the equations of motion in a cylindrical coordinate system gives rise to a singularity for $r=0$. Since the radial velocity v_r is the only one that is evaluated at the axis, singularity problems can be avoided by introducing the vector $\mathbf{w}=(rv_r, v_\theta, v_z)$ instead of $\mathbf{v}$. The equations of motion for $\mathbf{w}$ are then discretized in time; the viscous term is calculated implicitly by using a Crank–Nicolson technique, while the nonlinear and buoyancy terms are calculated explicitly using a third-order Runge–Kutta scheme. This leads to a second-order accuracy for the time advancement. A more detailed description of the numerical scheme can be found in Verzicco and Orlandi.[22]

All the runs presented here are performed using 128 grid points in both the r and the z direction. The grid convergence has been checked by performing simulations with double resolution (256^2) and half resolution (64^2). It was found that the flow is well resolved when 128^2 grid points are used and the results of the computation seem indistinguishable from a run with 256^2 grid points. Another check has been performed on the assumption that the flow remains axisymmetric during the computation: it was found that a fully three-dimensional simulation (with 128^3 grid points) yielded the same results as the corresponding axisymmetric computation and revealed that the flow indeed remained axisymmetric. Note that all these checks have been performed for the highest Reynolds number that we used (Re=2000). The cylindrical computational domain is bounded by a no-slip bottom and stress-free upper and lateral walls. It has been checked by runs with a larger domain in the radial sense that the finiteness of the domain in the radial direction did not affect the results.

For the simulations in a stratified fluid, which will be discussed in Sec. V, the equations of motion are solved in the Boussinesq approximation. The Boussinesq approximation implies that the pressure p and fluid density ρ can be expanded around a basic state, described by p_0 and ρ_0, as

$$p = p_0 + p', \quad \rho = \rho_0 + \rho'. \tag{17}$$

If the perturbations p' and ρ' around the basic state are small, we may assume that the density perturbation is only important in the gravitational term of the Navier–Stokes equation. The equations of motion that have to be solved then take the following form:

$$\frac{\partial \mathbf{v}}{\partial t} + (\mathbf{v}\cdot\nabla)\mathbf{v} = -\nabla p' - \frac{1}{\mathrm{Fr}^2}\rho' \mathbf{e_z} + \frac{1}{\mathrm{Re}}\nabla^2 \mathbf{v}, \tag{18}$$

$$\frac{DS}{Dt} = \frac{1}{\mathrm{Sc\,Re}}\nabla^2 S, \tag{19}$$

with S the salinity and $\mathbf{e_z}$ the unit vector in the z direction. The quantity ρ' is the density perturbation. It will be assumed that the density ρ is linearly proportional to the salinity as $\rho = \alpha S$. Three nondimensional parameters have been introduced in (18) and (19): the Froude number Fr, the Reynolds number Re, and the Schmidt number Sc, which are defined as

$$\mathrm{Fr} = \sqrt{\frac{\omega^2 L \rho_0}{g\Delta\rho}}, \quad \mathrm{Re} = \frac{L^2\omega}{\nu}, \quad \mathrm{Sc} = \frac{\nu}{\kappa}, \tag{20}$$

respectively. The quantities ω and L represent typical values for the vorticity and horizontal length scales in the flow, ρ_0 a typical value for the density, $\Delta\rho$ is a typical density difference, and κ is the diffusivity of the stratifying agent. A more precise definition of ω and L will be given in the next section.

In our simulations, the density perturbation from the basic state will not exceed 10%. It is assumed that for this value the Boussinesq approximation can be applied successfully.[23]

IV. NUMERICAL SIMULATIONS OF VORTICES IN A HOMOGENEOUS LAYER OF FLUID

The numerical simulations that are presented in this section will provide data that allows us to analyze the quasi-two-dimensionality of vortices in shallow fluid layers. The parameters that will be varied are the fluid depth H (or, equivalently Re_λ) and the ordinary Reynolds number Re. At

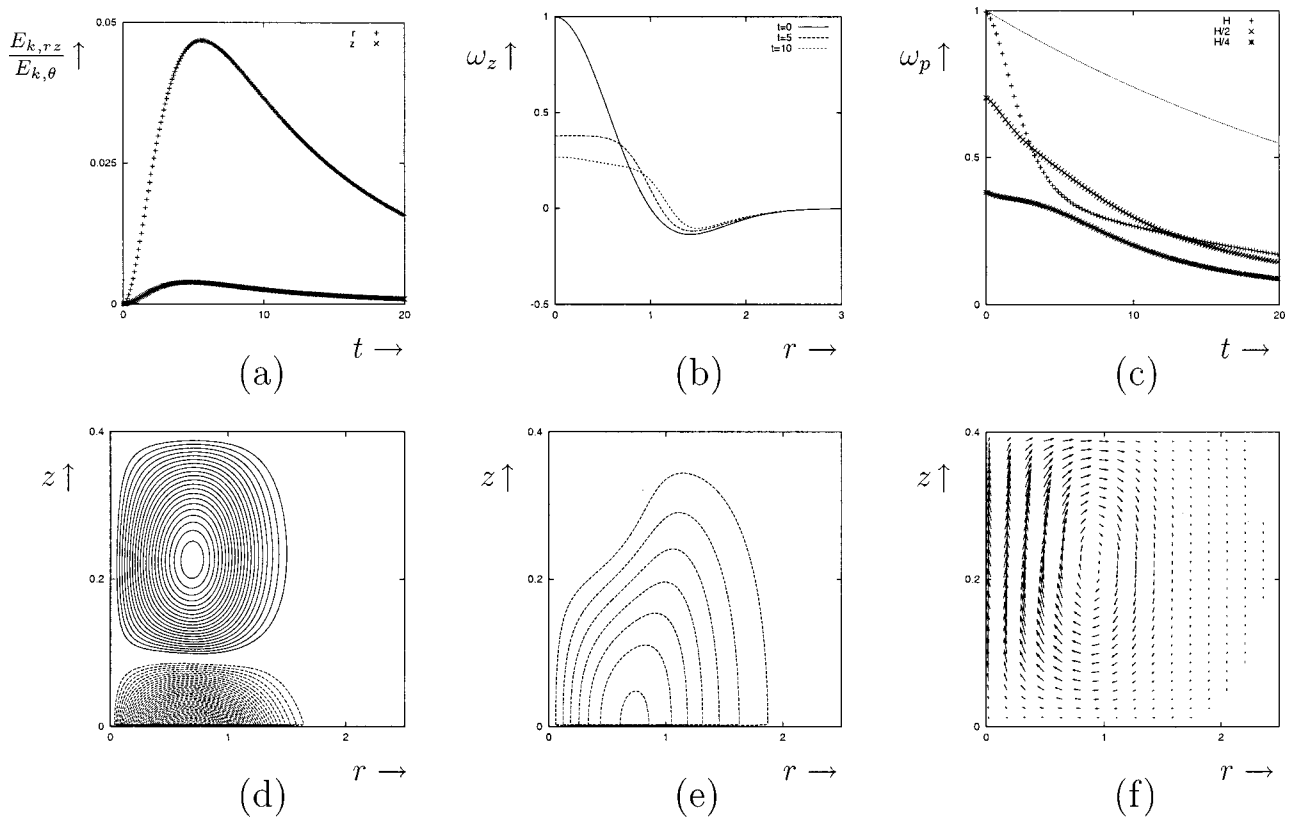

FIG. 2. Results of a numerical simulation with aspect ratio $\mu=0.20$ and Re$=500$. Shown are (a) the time evolution of the kinetic energy of the secondary flow, (b) time evolution of the vorticity profile $\omega_z(r)$ at the free surface, (c) the decay of the peak vorticity ω_p at three different levels, where the line represents (23), (d) contours of ω_θ (contour spacing $\Delta\omega_\theta=0.02$), (e) contours of ω_r (contour spacing $\Delta\omega_r=0.10$), and (f) velocity vectors in the (r,z) plane.

the end of this section, a regime diagram will be presented that shows in which region of the (Re,Re$_\lambda$) parameter space a flow can be considered as Q2D.

First, the dynamics and the 3D structure of a vortex will be analyzed in more detail for one specific case and we will discuss a way to characterize quasi-two-dimensionality in a quantitative fashion. Then, the effects of variation of the fluid depth H (or Re$_\lambda$) and the variation of the Reynolds number Re will be described separately. Finally, the obtained regime diagram will be presented.

As an initial condition, a purely azimuthal flow field is taken, with a shielded Gaussian vorticity distribution and a vertical profile that is sine-like, as described by the diffusion model in Sec. II. The complete initial condition is given by Eq. (10) with $a_0=1$ and $r_0=1$ for $t=0$,

$$v_\theta(r,z)=\frac{r}{2}\exp(-r^2)\sin\left(\frac{\pi z}{2H}\right). \tag{21}$$

In the first set of simulations presented below, the Reynolds number was Re$=500$, which is a typical value for several of the laboratory experiments that have been reported in literature. The Reynolds number is defined here as $\mathrm{Re}=L^2\omega_p/\nu$. The typical value for the vorticity is the initial peak vorticity ω_p at the axis $(r=0)$. As a typical horizontal length scale, the radius L, where the vorticity profile changes sign, is taken. The quantities a_0 and r_0, which determine the initial amplitude and radius of the vortex in (10), are thus used to nondimensionalize time and space. In most of the simulations presented here $\omega_p=1$ and $L=1$ so that $\mathrm{Re}=\nu^{-1}$.

The assumption made in the diffusion model, neglecting the higher-order modes of the axial–temporal solution (5), has been checked here for several situations. For low values of the fluid depth H, it was found that for other vertical velocity profiles, but still satisfying the boundary conditions, a rapid relaxation toward the solution given by (6) is observed. We may thus conclude that it is reasonable to use a sine-like vertical profile for the initial condition.

A. Dynamics and 3D structure of vortex flows: Characterization of quasi-two-dimensionality

Figure 2 presents the results for a simulation of a vortex with aspect ratio $\mu=0.20$. The height-to-width aspect ratio is defined as $\mu=H/d$, where $d=2L$. It is introduced only to provide a quick picture of the ratio of the vertical and horizontal dimensions of the vortex. Note that the aspect ratio is not a new nondimensional parameter. It depends on Re and Re$_\lambda$ as $\mu\sim(\mathrm{Re}_\lambda/\mathrm{Re})^{1/2}$.

The first quantity that will be considered is the magnitude of the kinetic energy of the secondary flow. For each component of the velocity v_i, where $i=(r,\theta,z)$ denotes the specific component, the kinetic energy is defined as

$$E_{k,i}=2\pi\int_0^H\int_0^R\frac{1}{2}\rho(z)v_i^2(r,z)r\,dr\,dz, \tag{22}$$

where H represents the total fluid depth and R the radius of the computational domain. For the simulations discussed in this section $\rho(z)=\rho$ is constant. In the next section we will discuss the evolution of vortex flows in a two-layer stratified system, where ρ will depend on the axial coordinate z.

We will discuss the time evolution of the values of $E_{k,r}$ and $E_{k,z}$ with respect to the value of the kinetic energy of the azimuthal main flow $E_{k,\theta}$. Hereafter, these ratios will be referred to as $q_r=E_{k,r}/E_{k,\theta}$ and $q_z=E_{k,z}/E_{k,\theta}$, respectively. In Fig. 2(a), these quantities are plotted as a function of time. At $t=0$, the kinetic energies $E_{k,r}=0$ and $E_{k,z}=0$, according to the initial condition. It is then observed that these energies first grow in time, indicating that a secondary circulation is set up inside the vortex. Afterward, due to the overall decay of the vortex structure, the secondary circulation will also weaken in time. The maximum values of the quantities q_r and q_z are reached at $t\simeq 5$.

One of the effects of the recirculation is clearly observed in Fig. 2(b), where the radial profile of axial vorticity $\omega_z(r)$ at the free surface is shown for three different times ($t=0$, $t=5$, and $t=10$). It can be seen that the vorticity profile deforms as time proceeds: the core of the vortex seems to relax toward a state of solid-body rotation. This deformation, caused by a 3D redistribution of axial vorticity, can only be a consequence of the recirculation in the (r,z) plane. In case of a Q2D flow, as described by the model in Sec. II, no deformation of the profile would occur and the vorticity profiles could be scaled in time.

Another way to examine 3D effects on the evolution of the vortex is to monitor the peak vorticity $\omega_p(t)$, which is located at the axis ($r=0$). Initially, the peak vorticity corresponds to the maximum axial vorticity $\omega_z=1$. The results of the computation are shown in Fig. 2(c), where the peak vorticity is plotted as a function of time at three different levels inside the vortex, being $h=H$ (free surface), $h=H/2$, and $h=H/4$. At the free surface ($h=H$), the initial peak vorticity $\omega_p|_{t=0}=1$, and subsequently decreases with height with a sine-like dependence until $\omega_p=0$ at the bottom, which is the boundary condition for the axial vorticity at the bottom. If the flow were Q2D, the decay would be uniform with respect to the vertical position z in the fluid column: rescaling the vorticity profiles with $\sin(\pi z/2H)$ would yield the same decay behavior. The solid line in Fig. 2(c) represents the expected decay of the peak vorticity at the free surface according to the diffusion model, which is given by

$$\omega_p(t)=\frac{\exp(-\lambda t)}{(1+4\nu t)^2}. \tag{23}$$

For the case with $\mu=0.20$, it can be seen that the actual decay of ω_p at the free surface differs significantly from the prediction based on the model, and besides that, it is observed that the decay is not uniform in z: the peak vorticity at the free surface even decreases below the value of the peak vorticity at $h=H/2$ for $4<t<12$. The enhanced decay of the peak vorticity at the free surface, and also the deformation of the vorticity profile, is caused by the secondary circulation, since the secondary flow transports low-amplitude axial vorticity, which is located near the bottom and near the axis, upward.

In order to give a complete picture of the 3D structure inside the vortex, contour plots of ω_θ and ω_r, which provide useful additional information about the secondary flow, are given for $t=5$ in Figs. 2(d) and 2(e), respectively. Here, solid lines represent contours of negative vorticity and dashed lines contours of positive vorticity. The velocity field at $t=5$ in the (r,z) plane, which is closely related with the azimuthal vorticity ω_θ, is shown in Fig. 2(f). It is observed that one large recirculation cell is present inside the vortex. The flow of the recirculation is directed toward the axis near the bottom, upward near the axis, and away from the axis near the free surface. Note that the largest velocity vectors in the (r,z) plane are usually located near the axis. From these data, it can also be concluded that the influence of the secondary circulation should be significant, since ω_θ is of the same order of magnitude as ω_z.

Based on the results of the simulation with $\mu=0.20$, two criteria will be introduced for characterizing the quasi-two-dimensionality in a quantitative fashion. The first one is related to the kinetic energies $E_{k,r}$ and $E_{k,z}$ of the secondary flow, compared to the kinetic energy of the azimuthal flow field $E_{k,\theta}$. It will be assumed that the flow behaves Q2D if

$$q_r(t)=\frac{E_{k,r}(t)}{E_{k,\theta}(t)}\leqslant 0.01, \quad q_z(t)=\frac{E_{k,z}(t)}{E_{k,\theta}(t)}\leqslant 0.01, \tag{24}$$

stating that the values of $E_{k,r}$ and $E_{k,z}$ should not exceed 1% of the value of $E_{k,\theta}$. In other words, the secondary motion in the (r,z) plane should be at least two orders of magnitude smaller than the azimuthal flow in terms of the kinetic energies. This criterion seems rather strict; it was found, however, that a value of the kinetic energy of the secondary flow that measures 1% of the kinetic energy of the azimuthal flow, corresponds to maximum values of the velocities v_r and v_z that are roughly only *one* order of magnitude smaller than the maximum in v_θ. In the first simulation with $\mu=0.20$, the criterion (24) is clearly not satisfied, since the maximum value of q_r almost measures $q_r=0.05$ [see Fig. 2(a)].

The condition (24), which concerns the kinetic energy of the secondary flow, is directly associated with the complete 3D flow field. The second criterion that will be used is related to the shape of the vorticity profile at the free surface [see Fig. 2(b)]. Since experimental velocity and vorticity fields are usually evaluated at the free surface, it is important to measure the effect of the secondary circulation there. We will measure this by evaluating the enstrophy Z at the free surface, which is here defined as

$$Z=\int\int_A \omega_z^2 da=2\pi\int_0^R \omega_z^2 r dr, \tag{25}$$

where A represents the area of the free surface and R the radius of the computational domain. The second criterion states that the flow can be considered as Q2D if the ratio Q, which is defined as

$$Q=\frac{\int_0^R[\omega_z'(r',0)-\omega_z'(r',t)]^2 r dr}{\int_0^R \omega_z'^2(r',0) r dr}, \tag{26}$$

does not exceed 0.10. The quantity $\omega_z'(r',t)$ represents the rescaled vorticity profile with respect to its amplitude and radius. The deformation of the vorticity profile is thus characterized by comparing the shape of a rescaled profile at time t with the initial condition, which also serves as a weight function. The flow will now be considered Q2D if both conditions (24) and (26) are fulfilled.

For the case with $\mu=0.20$, as discussed above, this criterion is not satisfied either, since $Q=0.97$. Note that the time evolution of Q will not be discussed here. In most of the cases, the deformation of the vorticity profile is irreversible and Q increases in time. The value of Q will be calculated at $t=5$, which will be assumed to give a reasonable representation for the complete flow evolution. No additional criteria will be formulated concerning ω_θ, ω_r, or the evolution of ω_p, since this would not reveal any new information which is essentially different from the criteria that have already been formulated.

B. Variation of the fluid depth

In the set of simulations presented below the vortex aspect ratio will be varied in order to determine the effect of the fluid depth on the 3D structure and the decay properties of the flow. While L was kept constant, five different fluid depths H were taken, resulting in aspect ratio values of $\mu=0.50$, 0.20, 0.15, 0.10, and 0.05. The corresponding values of Re_λ are given by $\mathrm{Re}_\lambda=203$, 32.5, 18.2, 8.1, and 2.0, respectively. The value of Re_λ is thus systematically decreased for fixed (ordinary) Reynolds number Re. The influence of Re will be discussed in the next part of this section. The case with $\mu=0.20$ has already been discussed above. The magnitude of the kinetic energy of the secondary flow, the evolution of the vorticity profiles at the free surface and the decay of the peak vorticities will now be shown for three other aspect ratios. These data should be compared to the case of $\mu=0.20$, which has been discussed in the previous part of this section.

Increasing the aspect ratio to $\mu=0.50$ has a dramatic effect on the evolution of the vortex, as can be concluded from the results presented in Fig. 3(a). At $t=10$, the values of q_r and q_z have reached a magnitude of $\sim$15% and $\sim$5%, respectively. It follows that in this case, as in the previous case with $\mu=0.20$, it is clearly not justified to consider the flow as being Q2D. The profound effect of the intense secondary circulation can be observed in the evolution of the vorticity profile at the free surface and the decay of the peak vorticities, as shown in Fig. 3(a). The strong deformation of the vorticity profile results in a maximum axial vorticity, which is no longer located at the center of the vortex, but is instead shifted outward. This shift is a direct consequence of the outward advection of axial vorticity at the free surface due to the secondary circulation. The quantity Q measures $Q=1.63$ in this case, which is substantially larger than in the case of $\mu=0.20$. It is also shown that the peak vorticities do not show any uniform decay at all. In fact, at $t=5$ the peak vorticities at level $H/2$ and $H/4$ have become larger than the vorticity at the free surface, which is strongly reduced during the initial stage of the evolution.

Decreasing the fluid depth, so that the aspect ratio of the vortex reduces to $\mu=0.10$ [shown in Fig. 3(b)] or $\mu=0.05$ [shown in Fig. 3(c)] shows a completely different scenario. Obviously, the values of the kinetic energies $E_{k,r}$ and $E_{k,z}$, divided by $E_{k,\theta}$, are now much smaller than in the previous cases. For $\mu=0.10$ a maximum value for q_r is reached at $t\simeq 2$ of 0.007, while for $\mu=0.05$ this maximum measures only 0.0005. The effect on the evolution of the vorticity distribution is clear: scaling the vorticity profiles with their value at $r=0$ (not shown), reveals that the profile does not deform significantly for $\mu=0.10$ and can be scaled almost perfectly for $\mu=0.05$. This is an indication that the flow maintains its two-dimensional character and secondary circulations are much weaker. In quantitative terms, the value of Q decreases to $Q=0.093$ for $\mu=0.10$, which is roughly an order of magnitude smaller than in the case of $\mu=0.20$. For $\mu=0.05$ it is further reduced to $Q=0.0043$. According to our criteria, the flows can thus be considered as Q2D in these cases. The decrease of the aspect ratio to $\mu=0.05$ leads to a decay scenario that almost perfectly fits with the diffusion model, as can be concluded from Fig. 3(c). For $\mu=0.10$, the diffusion model would be a good approximation. However, in some experimental situation, where one wishes to study the evolution of flows for a reasonable amount of time, a situation like for $\mu=0.05$ is not preferable, since the damping is too large.

C. Variation of the Reynolds number

In the simulations discussed above, the influence of the fluid depth H (or, equivalently, Re_λ) on the evolution of the vortex flow has become clear for a fixed value of the Reynolds number Re. In general, it can be concluded that the flow loses its Q2D character for larger fluid depths. The influence of the Reynolds number Re, associated with lateral diffusion, on the 2D character of the flow has not been discussed yet. For all the five fluid depths, the Reynolds number has been varied in the range $125\leqslant \mathrm{Re}\leqslant 2000$. In Fig. 4, a typical set of two simulations is presented to illustrate its basic effect. These runs should be compared to the simulation with $\mu=0.20$ and $\mathrm{Re}=500$, as discussed in the first part of this section. Two cases will be studied: the evolution of the flow with a lower Reynolds number [$\mathrm{Re}=125$, shown in Fig. 4(a)] and a higher Reynolds number [$\mathrm{Re}=2000$, shown in Fig. 4(b)]. The Reynolds number was changed here by multiplying the radius L of the vortex by a factor of $\frac{1}{2}$ and 2, respectively. The aspect ratios are then given by $\mu=0.40$ and $\mu=0.10$, respectively. The value of Re_λ is, of course, not affected by the adjustment of the horizontal scale of the flow. Note that it is not useful to change the kinematic viscosity ν while keeping the dimensions of the vortex constant. This would results in an effectively different fluid depth, since the damping parameter λ includes the viscosity ν.

Considering the kinetic energy of the secondary flow, the evolution of the vorticity profile at the free surface, and the decay of the peak vorticities, it can be concluded that

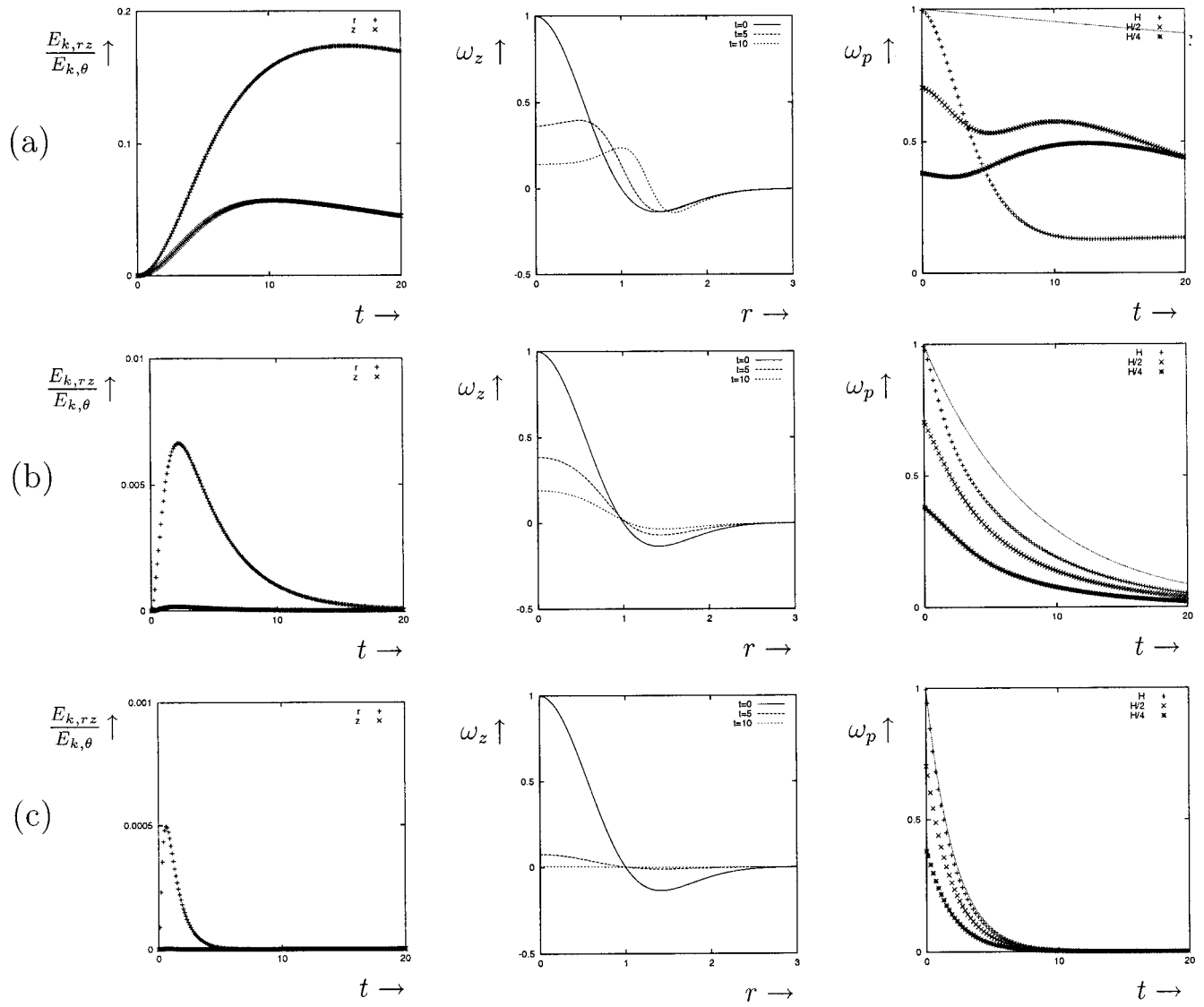

FIG. 3. Numerical simulations in a homogeneous layer of fluid with Re=500. Shown are the time evolution of the kinetic energy of the secondary flow, the time evolution of the vorticity profile $\omega_z(r)$ at the free surface and the decay of the peak vorticity ω_p at three different levels, where the lines represent (23), for (a) $\mu=0.50$, (b) $\mu=0.10$, and (c) $\mu=0.05$.

decreasing the Reynolds number two-dimensionalizes the flow, while for an increase of the Reynolds number the flow loses its Q2D character. For Re=125, the maximum value of q_r roughly measures 0.03, while for Re=2000 it increases up to 0.05. The deformation of the vorticity profile is also significantly reduced for Re=125, compared to the case of Re =2000. In terms of the quantity Q, the result is that for Re=125, Q is reduced to $Q=0.44$ while for Re=2000 its value measures $Q=1.19$. The decay of the peak vorticities appears to be more uniform in the case of Re=125.

In Sec. II, it was mentioned that the dynamics of very small scales are probably not well described by the diffusion model due to 3D effects. In order to study this in more detail a simulation has been performed with a very small L so that Re=1. The aspect ratio is then given by $\mu=5.0$. The results are presented in Fig. 5, where the time evolution of the kinetic energy and the evolution of the rescaled vorticity profile is shown. It is observed this small-scale vortex behaves essentially Q2D, according to the values of the kinetic energies. A clear lateral expansion is also observed since lateral diffusion plays an important role in the evolution.

Note that it is quite surprising that an effective increase of the aspect ratio μ of the vortex leads to a more two-dimensional character of the flow. Apparently, the aspect ratio itself is not an essential parameter for the evolution of the flow. Remarkably, the flow seems to be governed by Re and Re_λ separately. The physical explanation for this phenomenon is most likely that for higher Reynolds number, and thus for a *lower* aspect ratio, the nonlinear advective term in the Navier–Stokes equation becomes more and more important. In other words, the dynamical effect of changing the Reynolds number is apparently more important than the corresponding geometrical effect.

The effect of variation of Re_λ and Re separately has become clear from the simulations discussed above. As mentioned before, several additional simulations have been performed in order to construct a regime diagram for flows in a shallow layer of fluid. This diagram concerns the quasi-two-

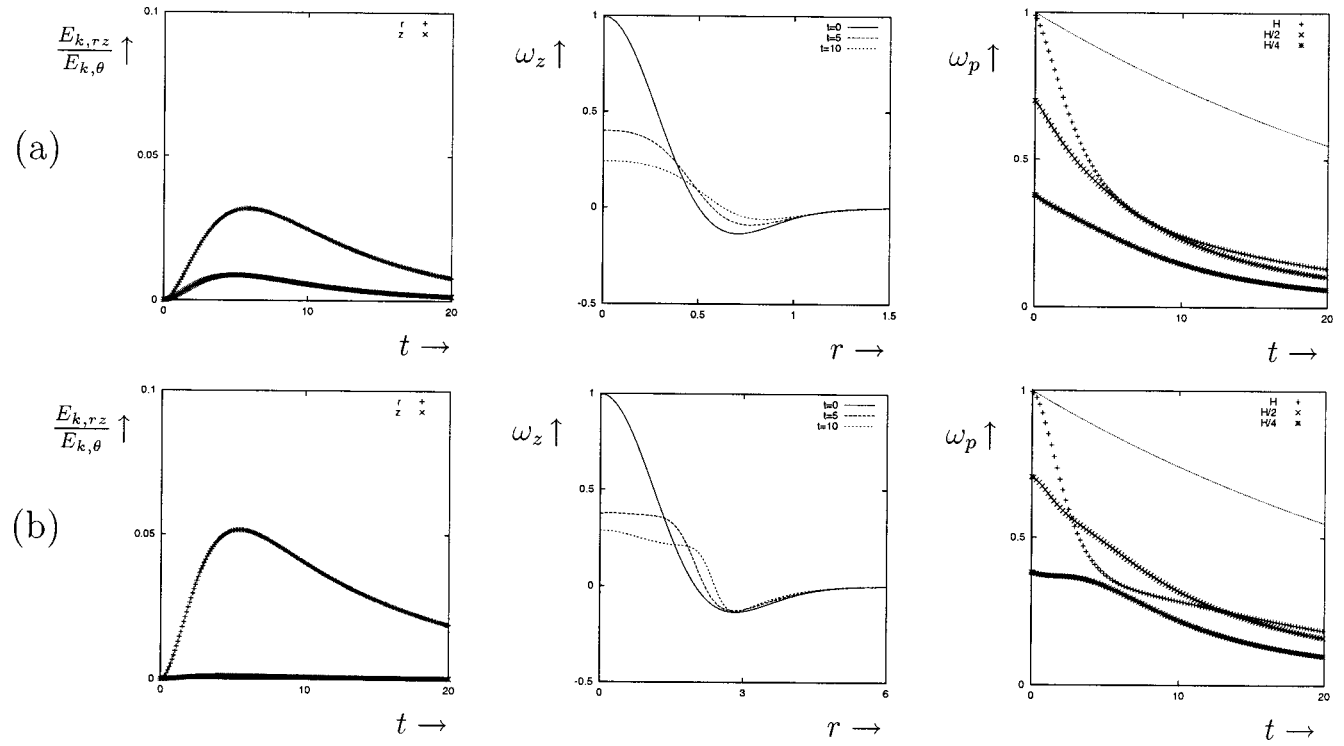

FIG. 4. Numerical simulations in a homogeneous layer of fluid. Shown are the time evolution of the kinetic energy of the secondary flow, the evolution of the vorticity profile $\omega_z(r)$ at the free surface, and the decay of the peak vorticity ω_p at three different levels, where the lines represent (23), for (a) Re=125 (μ=0.40) and (b) Re=2000 (μ=0.10).

dimensionality, using the criteria that we have defined, as a function of Re and Re_λ. The additional simulations will not be discussed in detail here. The diagram is shown in Fig. 6. The simulated flows that are indicated by a + should be considered 3D, while the simulations indicated by a $\times$ represent a quasi-2D flow, according to our criteria. The dashed line represents an estimation of the borderline between Q2D and 3D flows, and was determined by using the results of the simulations. Below the dashed line, the flow can thus be considered as Q2D, above the line it should be considered 3D. A clear region can thus be distinguished in the ($\mathrm{Re},\mathrm{Re}_\lambda$) parameter space, where the flow can be considered as Q2D, according to our criteria.

V. NUMERICAL SIMULATIONS OF VORTICES IN A STRATIFIED FLUID

Basically, the simulations discussed in this section are performed using the same parameters ($\mathrm{Re},\mathrm{Re}_\lambda$) and initial condition as in the runs presented in the previous section. The difference with the runs of the previous section is that instead of a homogeneous fluid layer now a two-layer stratified system is taken. We will thus construct a similar regime diagram for vortex flows in a stratified fluid and make a comparison with the case of a single layer. The density difference in the two layers is 10%, corresponding to a Froude number of Fr=1.0. In the initial condition, the density is

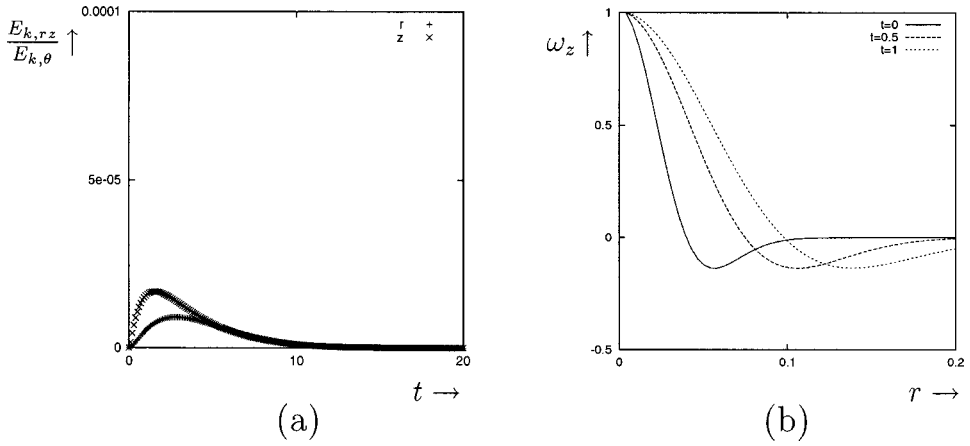

FIG. 5. Evolution of a small-scale vortex structure. Shown are (a) the time evolution of the kinetic energy of the secondary flow and (b) the evolution of the vorticity profile $\omega_z(r)$ [rescaled with $\omega_z(0)$] at the free surface.

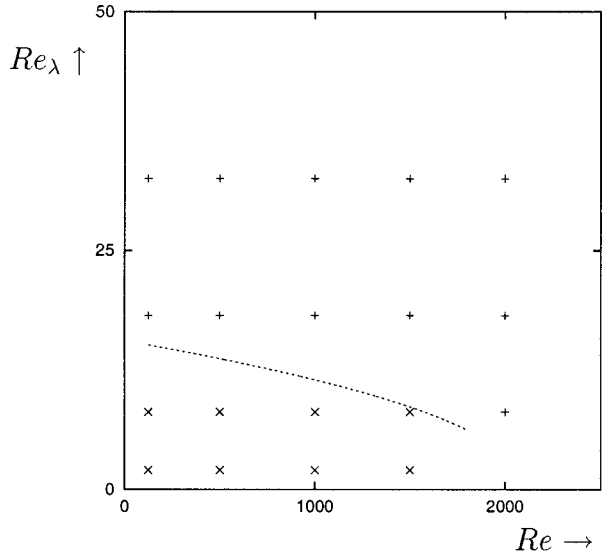

FIG. 6. Regime diagram for flows in a single shallow layer of fluid as a function of Re and Re_λ. Below the dashed line, the flow can be considered as Q2D; above the line it should be considered 3D.

adjusted from its value in the lower layer to its value in the upper layer in a vertical region that spans 10% of the total fluid depth. Due to diffusion of the stratifying agent the gradients in the step-like density profile $\rho(z)$ will gradually be smeared out. The Schmidt number in all cases is $\mathrm{Sc}=700$, which is representative for the case that the stratifying agent is salt (NaCl solution), which is commonly used in laboratory experiments. On the time scales of the simulations discussed here ($0<t<20$), the two-layer system is nearly unaffected. On longer time scales, the density profile would evolve toward an almost linear one [$\rho(z)\sim z$]. Note that the density gradient at the bottom and free surface equals $\partial\rho/\partial z=0$ for all times, owing to the no-flux condition for passive scalar at the upper and lower boundaries.

Note that the vertical structure and the decay properties of vortices in a two-layer stratified system can be approximated by the model of a vortex in a single layer of fluid, as presented in Sec. II. A difference arises in the value of the kinematic viscosity ν in the upper and lower layer, which depends on the density ρ. As a consequence, the boundary condition at the interface yields $\nu_1\rho_1(\partial u_\theta/\partial z)|_1 = \nu_2\rho_2(\partial u_\theta/\partial z)|_2$, so that a slight kink is expected in the vertical velocity profile at the rather sharp interface that has been used. Another (dynamical) difference that arises is the following: from the cyclostrophic and hydrostatic balances, it can be understood that, apart from a small deformation of the free surface, the density interface will be deflected upward in the core of the vortex. The reason for this is a lower pressure in the upper layer due to the higher values of the azimuthal velocity there.

The remaining part of this section is organized in a similar way as the previous one. First, the dynamics and 3D structure of a vortex in a two-layer stratified fluid is discussed for one specific situation ($\mu=0.20$, as in the case of a single layer). Then, the variation of the fluid depth and the Reynolds number will be discussed and the obtained regime diagram will be presented. Finally, we will briefly analyze some experiments that have been reported in the literature within the context of our results.

A. Dynamics and 3D structure of a vortex in a stratified fluid

The first simulation that is presented here should be compared to the first one in the previous section. The aspect ratio of the vortex equals $\mu=0.20$. When this simulation is compared to the corresponding run in a homogeneous layer of fluid, some remarkable differences are found. The results of the calculation are presented in Fig. 7. First, the values of the kinetic energies of the secondary flow $E_{k,r}$ and $E_{k,z}$, with respect to $E_{k,\theta}$ [shown in Fig. 7(a)], are approximately a factor of 4 smaller than in the case of a homogeneous layer of fluid. This obviously corresponds to a much weaker secondary circulation. The deformation of the radial vorticity profile at the free surface is almost absent here, as can be observed in Fig. 7(b). From Fig. 7(c), where the time evolution of the peak vorticities is shown, it can be concluded that the decay is also significantly reduced. It can be seen that the decay for longer time scales ($t>8$) approaches the decay as expected by the diffusion model. According to the formulated criterion in terms of the enstrophy, this case could be considered as Q2D, in contrast to the case of a single layer. The quantity Q measures $Q=0.044$, which is very small compared to the value of $Q=0.97$ for the case of a homogeneous layer. However, the value of q_r shows a slight excess of the 0.01 norm for $1<t<3$. This means that the flow in this case behaves on the verge of quasi-two-dimensionality.

The recirculation pattern is remarkably different, which is shown in Figs. 7(d) and 7(e) by contours of ω_θ and ω_r and in Fig. 7(f) by velocity vectors in the (r,z) plane for $t=5$. Instead of one large recirculation cell, now a multiple-cell structure of counter-rotating circulations is observed. Note that this pattern is not stationary in time. The alternating upward and downward motions near the interface are believed to be associated with internal waves. Although the pattern is more complex than for the homogeneous case, it is also much weaker and, as a consequence, its influence on the behavior of the flow is less pronounced.

It is an important question why the decay is reduced significantly in the upper layer. In the system we discuss here, there are several mechanisms to establish this. The main reason for the reduced decay is that the flow in the upper layer is effectively shielded from the lower layer due to the stratification. The secondary circulation is therefore much weaker, which prevents the advection of low-amplitude axial vorticity from the lower layer to the upper layer. Another mechanism, which is less important, is the following: by using different densities, the kinematic viscosity of the upper layer changes. As a consequence, the diffusion in lateral and vertical sense acts at different time scales. Since $\nu\sim\rho^{-1}$, the kinematic viscosity decreases for increasing density. Since the density difference is only 10%, it is expected that this effect is very weak.

A third mechanism could be related to the deformation of the density interface. An amount of potential energy is

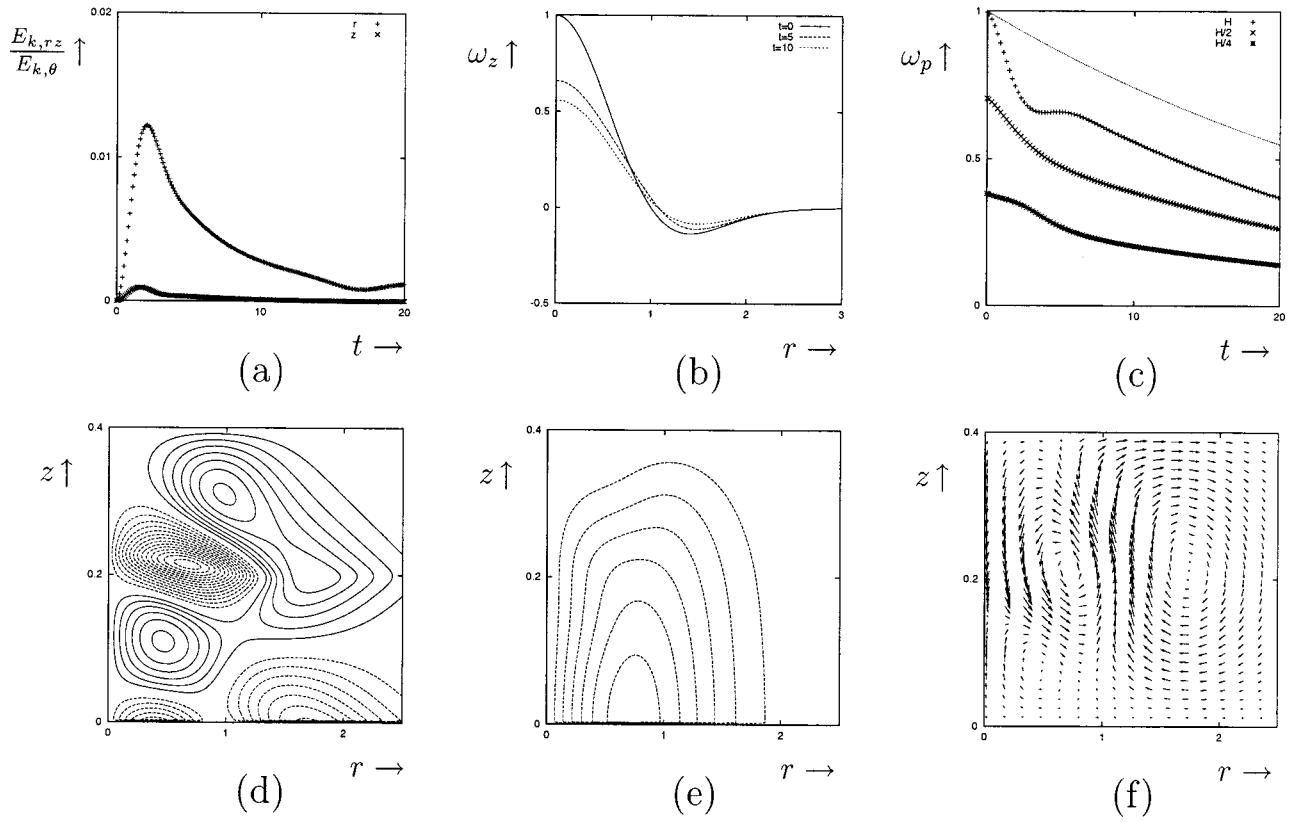

FIG. 7. Results of a numerical simulation in a stratified fluid with $\mu=0.20$ and Re=500. Shown are (a) the time evolution of the kinetic energy of the secondary flow, (b) time evolution of the vorticity profile $\omega_z(r)$ at the free surface, (c) decay of the peak vorticities ω_p at three different levels, where the line represents (23), (d) contours of ω_θ (contour-spacing $\Delta\omega_\theta=0.02$), (e) contours of ω_r (contour spacing $\Delta\omega_r=0.10$), and (f) velocity vectors in the (r,z) plane.

stored when the interface is lifted in the first time units. After the interface has risen to its maximum height, the interface relaxes to its original position. The potential energy, which has been stored in this way, will be released if the interface relaxes to its undisturbed position. This is accompanied by stretching of the vortex column above the interface and compression of the vortex beneath the interface. Initially, when the interface rises, the vortex column above the interface is compressed whereas the vortex beneath the interface is stretched. In Fig. 7(c), it is indeed observed (for $0<t<4$) that the peak vorticity at the free surface shows an enhanced decay, while for $h=H/4$ the decay of the peak vorticity is slightly reduced. For $4<t<7$, it can be seen that the decay at the free surface is reduced, while it is slightly enhanced for $h=H/4$. However, a separate calculation of the kinetic energy in the upper and lower layer (not shown) reveals only a slight asymmetry in the decay of these layers. Apparently, this mechanism is not important in terms of the kinetic energy. A substantial part of the available potential energy is most likely transferred into kinetic energy by the excitation of internal waves.

B. Variation of the fluid depth and the Reynolds number

When the total fluid depth is varied in the stratified case, the same phenomena are observed as in the case of a homogeneous layer. Increasing the aspect ratio to $\mu=0.50$ results in a loss of two-dimensionality of the flow field, although this effect is much more dramatic in case of a homogeneous layer. This can be concluded from the maximum values of q_r and q_z, the evolution of the vorticity profiles at the free surface and the decay of the peak vorticities, as shown in Fig. 8(a). An interesting feature of flows in a stratified system is revealed by the decay of the kinetic energies. It is observed that the values of q_r and q_z decrease with a wavelike disturbance. These disturbances are most likely caused by the excitation of internal waves, whose presence is apparently more pronounced for larger fluid depths.

Decreasing of the fluid depth also in this case leads to a more Q2D character of the flow. In Fig. 8(b), the results are shown for a simulation with $\mu=0.10$, which can be considered as Q2D. For $\mu=0.05$ (not shown), the decay again perfectly fits the diffusion model. Note that in both cases no large differences are found with the case of a single layer. The calculated values of Q are $Q=0.022$ for $\mu=0.10$ and $Q=0.0035$ for $\mu=0.05$.

The Reynolds number has also been varied for the simulations presented in this section. As in the case of a single layer, the range of variation was $125\leqslant \mathrm{Re}\leqslant 2000$. Here, it was also observed that decreasing the Reynolds number two-dimensionalizes the flow, while for increasing Reynolds number, the flow loses its Q2D character. The runs for different Re, which allow us to construct a similar regime diagram as for the case of a single layer of fluid, will not be discussed in detail here. The diagram is shown in Fig. 9. The dividing line has been determined in the same way as for the

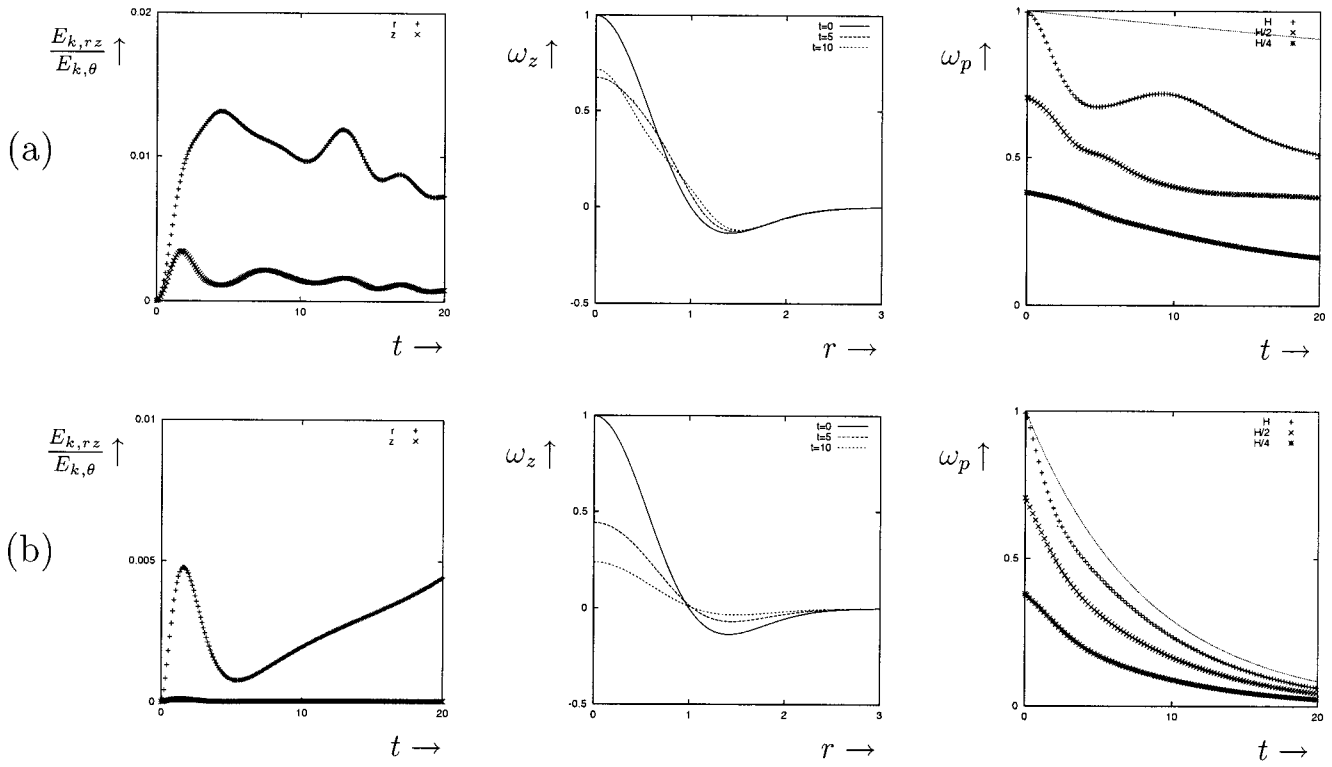

FIG. 8. Numerical simulations in a stratified fluid with Re=500. Shown are the time evolution of the kinetic energy of the secondary flow, the time evolution of the vorticity profile $\omega_z(r)$ at the free surface and decay of the peak vorticity ω_p at three different levels, where the lines represent (23), for (a) $\mu=0.50$ and (b) $\mu=0.10$.

homogeneous case. Below the dashed line, the flow can be considered as Q2D, above the line it should be considered 3D. It can be seen that the parameter regime where the flow can be considered Q2D is larger than in the case of a single layer. Especially for lower values of the Reynolds number, the range of fluid depths where the flow behaves Q2D is much bigger.

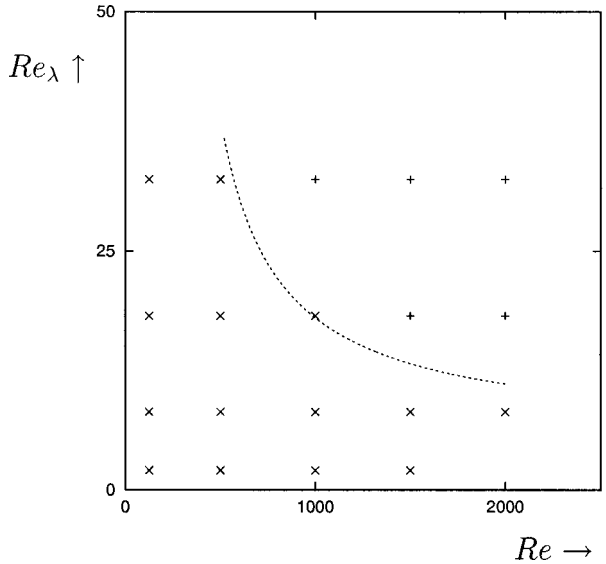

FIG. 9. Regime diagram for flows in a two-layer stratified fluid. Below the dashed line, the flow can be considered as Q2D; above the line it should be considered 3D.

Flows in shallow layers of fluid are commonly assumed to behave Q2D. We have formulated and tested criteria for the quasi-two-dimensionality of such flows. An analysis of the Q2D character of some thin-layer experiments that have been carried out by several authors (e.g., Antonova *et al.*,[11] Tabeling *et al.*,[12] and Paret *et al.*[16]) is thus worthwhile. To make a comparison between these experiments and our simulations, the absolute values of the fluid depth and a typical value for the peak vorticity, or some typical value for the velocity and length scale, has to be known for proper scaling of the flows. Unfortunately, none of the authors mentioned above provide all these values, so it is not possible to draw conclusions about the quasi-two-dimensionality of these experiments. It is thus unclear whether 3D effects in laboratory experiments are small enough to ensure the validity of the quasi-2D approximation. Our method for determining the quasi-two-dimensionality could be applied in future studies.

VI. CONCLUSIONS AND DISCUSSION

Laboratory experiments aimed at studying the dynamics of vortices and two-dimensional turbulence have been performed in shallow layers of fluid. The geometrical confinement is then a commonly used argument for the flow to behave in a quasi-two-dimensional fashion. When these experiments are performed inside a container, a no-slip boundary condition applies to the bottom of the tank and a stress-free condition at the free surface. The no-slip boundary condition implies a vertical shear, which leads to secondary

circulations within the planar vortices. In this paper, the three-dimensional structure and the decay properties of vortices in such a system of shallow fluid layers have been studied numerically.

It has been found that for large fluid depths and large Reynolds number the flow loses its two-dimensional character. Effectively, this means that a significant secondary circulation is present. One of the effects of this recirculation is the deformation of the radial profile of axial vorticity. As a consequence, the decay of the vortices is no longer consistent with a Q2D diffusion model, which predicts that the vorticity profiles can be scaled when the flow can be considered as Q2D. For low values of Re and Re_λ, it has been found that the decay indeed perfectly fits the diffusion model. We were able to characterize the quasi-two-dimensionality in a quantitative fashion by considering the strength of the recirculations in terms of the kinetic energy and by characterizing the deformation of the vorticity profile. Furthermore, it is possible to construct a regime diagram to assess the validity of the Q2D approximation in the $(\mathrm{Re},\mathrm{Re}_\lambda)$ parameter space. It should be noted that the method here proposed for characterizing quasi-two-dimensionality could also be applied to vortices in rotating and/or stratified fluids in future studies.

It has also been found that vortices in a two-layer stratified fluid, compared to flows in a homogeneous layer, maintain their two-dimensional character for larger fluid depths. The decay of a vortex in a stratified fluid is also significantly reduced, compared to the case of a single layer. To summarize, the numerical simulations in this paper reveal that vortex structures in shallow layers of fluid can be considered as Q2D only under certain conditions, being a depth that is small enough and a Reynolds number that is not too large. It is worthwhile to note that the height-to-width aspect ratio is a confusing parameter if one considers quasi-two-dimensionality of shallow water flows: it was found that flows with a *higher* aspect ratio behave ''more 2D,'' if the fluid depth is the same. In other words, the dynamical effect of changing the Reynolds number is apparently more important than the corresponding geometrical effect.

Thus, laboratory experiments of this type can only be compared with (quasi-)two-dimensional models when certain conditions are fulfilled. With the method presented here, it should be possible to analyze several experiments that have been reported in the literature (and that were assumed to be 2D). However, we were not able to perform such an analysis, since not all the necessary parameters were known.

Although we have given a detailed description of the three-dimensional structure of decaying vortical flows, it is still an open question how the behavior will be modified in the case of forced vortical flows, for instance, in flows that are continuously forced electromagnetically. It is expected, however, that the basic features discussed in the preceding sections—the presence of recirculations, a loss of two-dimensionality for larger fluid depths, and larger Reynolds number—will not change significantly in the case of a forced system.

ACKNOWLEDGMENT

One of the authors (M.P.S.) gratefully acknowledges financial support from the Dutch Foundation for Fundamental Research on Matter (FOM).

[1] E. J. Hopfinger and G. J. F. van Heijst, ''Vortices in rotating fluids,'' Annu. Rev. Fluid Mech. **25**, 241 (1993).
[2] G. J. F. van Heijst and R. C. Kloosterziel, ''Tripolar vortices in a rotating fluid,'' Nature (London) **338**, 369 (1989).
[3] M. Beckers, R. Verzicco, H. J. H. Clercx, and G. J. F. van Heijst, ''Dynamics of pancake-like vortices in a stratified fluid: Experiments, model and numerical simulations,'' J. Fluid Mech. **433**, 1 (2001).
[4] J. B. Flór and G. J. F. van Heijst, ''Dipole formation and collisions in a stratified fluid,'' Nature (London) **340**, 212 (1989).
[5] S. R. Maassen, H. J. H. Clercx, and G. J. F. van Heijst, ''Decaying quasi-2D turbulence in a stratified fluid with circular boundaries,'' Europhys. Lett. **46**, 339 (1999).
[6] P. F. Linden, B. M. Boubnov, and S. B. Dalziel, ''Source–sink turbulence in a rotating stratified fluid,'' J. Fluid Mech. **298**, 81 (1995).
[7] J. Sommeria, ''Experimental study of the two-dimensional inverse energy cascade in a square box,'' J. Fluid Mech. **170**, 139 (1986).
[8] Y. Couder, ''Two-dimensional grid turbulence in a thin liquid film,'' J. Phys. (France) Lett. **45**, 353 (1984).
[9] H. Kellay, X-l. Wu, and G. I. Goldburg, ''Experiments with turbulent soap films,'' Phys. Rev. Lett. **74**, 3975 (1995).
[10] M. A. Rutgers, ''Forced 2D turbulence: Experimental evidence of simultaneous inverse energy and forward enstrophy cascade,'' Phys. Rev. Lett. **81**, 2244 (1998).
[11] R. A. Antonova, B. P. Zhvania, J. I. Nanobashvili, and V. V. Yan'kov, ''Vortices in a two-dimensional incompressible fluid,'' Bull. Acad. Sci. Georg. SSR **119**, 97 (1985) (translation from Russian).
[12] P. Tabeling, S. Burkhart, O. Cardoso, and H. Willaime, ''Experimental study of freely decaying two-dimensional turbulence,'' Phys. Rev. Lett. **67**, 3772 (1991).
[13] S. D. Danilov, F. V. Dolzhanskii, V. A. Dovzhenko, and V. A. Krymov, ''An advanced investigation of interaction of allocated quasi two-dimensional vortices,'' Chaos **6**, 297 (1996).
[14] F. V. Dolzhanskii, V. A. Krymov, and D. Yu. Manin, ''An advanced experimental investigation of quasi two-dimensional shear flows,'' J. Fluid Mech. **241**, 705 (1992).
[15] F. V. Dolzhanskii, V. A. Krymov, and D. Yu. Manin, ''Stability and vortex structures of Q2D shear flows,'' Usp. Fiz. Nauk **160**, 1 (1990).
[16] J. Paret and P. Tabeling, ''Experimental observation of the two-dimensional inverse energy cascade,'' Phys. Rev. Lett. **79**, 4162 (1997).
[17] J. Paret, D. Marteau, O. Paireau, and P. Tabeling, ''Are flows electromagnetically forced in thin stratified layers two-dimensional?'' Phys. Fluids **9**, 3102 (1997).
[18] B. Jüttner, D. Marteau, P. Tabeling, and A. Thess, ''Numerical simulations of experiments on quasi two-dimensional turbulence,'' Phys. Rev. E **55**, 5479 (1997).
[19] F. V. Dolzhanskii, ''Transverse structures of Q2D geophysical and MHD flows,'' Izv. Atmos. Ocean. Phys. **35**, 147 (1999).
[20] O. Paireau, P. Tabeling, and B. Legras, ''A vortex subjected to a shear: An experimental study,'' J. Fluid Mech. **351**, 1 (1997).
[21] R. C. Kloosterziel, ''On the large-time asymptotics of the diffusion equation on infinite domains,'' J. Eng. Math. **24**, 213 (1990).
[22] R. Verzicco and P. Orlandi, ''A finite difference scheme for direct simulation in cylindrical coordinates,'' J. Comput. Phys. **123**, 402 (1996).
[23] P. K. Kundu, *Fluid Mechanics* (Academic, New York, 1990).